Chemical Research in Toxicology

Article

pubs.acs.org/crt

CuO Nanoparticle Interaction with Human Epithelial Cells: Cellular Uptake, Location, Export, and Genotoxicity

Zhenyu Wang,*[,†] Na Li,[†] Jian Zhao,[‡] Jason C. White,[§] Pei Qu,[†] and Baoshan Xing*[,‡]

[†]College of Environmental Science and Engineering, Ocean University of China, Qingdao 266100, China

[‡]Department of Plant, Soil and Insect Sciences, University of Massachusetts, Amherst, Massachusetts 01003, United States

[§]Department of Analytical Chemistry, Connecticut Agricultural Experiment Station, New Haven, Connecticut 06511, United States

Supporting Information

ABSTRACT: The toxicity of CuO nanoparticles (NPs) to human lung epithelial (A549) cells was investigated in this study. CuO NPs (10−100 mg/L) had significant toxicity to A549 cells, whereas CuO bulk particles (BPs) showed much lower toxicity (24 h IC_{50}, 58 and 15 mg/L for CuO BPs and NPs, respectively). Transmission electron microscopic analysis demonstrated CuO NP entry into A549 cells and organelles, including lysosomes, mitochondria, and nucleus. Endocytosis was the primary pathway of CuO NPs uptake. CuO NPs (15 mg/L) induced mitochondrial depolarization, possibly mediated by reactive oxygen species (ROS) generation. Intracellular CuO NPs first generate ROS, which subsequently induces the expression of *p38* and *p53* and ultimately causes DNA damage (Comet assay). We confirm for the first time that the primary cytotoxic response is oxidative stress rather than DNA damage. A fraction of the CuO NPs was exported to the extracellular environment. In this study, centrifugal ultrafiltration tubes were successfully employed to determine the dissolved Cu^{2+} from CuO NPs in the cell medium. Dissolved Cu^{2+} ions contributed less than half of the total toxicity caused by CuO NPs, including ROS generation and DNA damage. This study provided useful data for understanding transport and toxicity of metal oxide NPs in human cells.

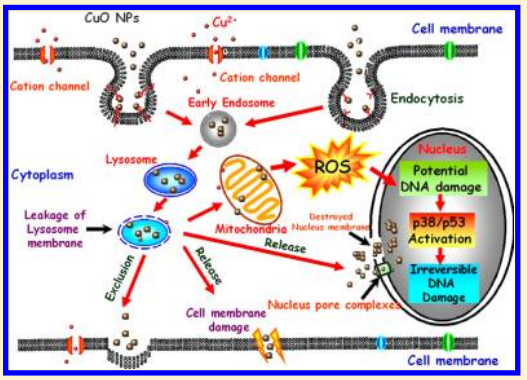

INTRODUCTION

Metal and metal oxide nanoparticles (NPs) are widely applied in personal care products,[1] catalysis,[2] optical and recording devices,[3] and water purification.[4] Recently, the toxicity of metal and metal oxide NPs on mammalian cells has been studied, and a number of researchers have found that metal and metal oxide NPs can generate oxidative stress and promote cytotoxicity.[5,6] However, critical issues such as intracellular localization, uptake and export mechanisms, and the precise mode of toxicity remain unclear.

Several studies have shown that oxidative stress plays a key role in cellular toxicity associated with metal (Ag) and metal oxide (ZnO, SiO_2) NPs exposure.[7−9] However, Eom and Choi[10] demonstrated that oxidative stress may not be the direct cause of the Ag NP cytotoxicity. Cellular signaling pathways were activated by Ag NPs, subsequently inducing DNA damage, cell cycle arrest, and apoptosis. Moreover, both Geiser et al.[11] and Ahamed et al.[12] observed that TiO_2 and Ag NPs, respectively, could be transported to the nucleus and directly interact with nuclear DNA/proteins. However, the sequence of events between oxidative stress and subsequent DNA damage (presumed primary response) under NP exposure is still unknown. The primary mode of particle uptake by cells has been shown to be energy-dependent endocytosis and macropinocytosis (especially for macrophages).[13,14] However, few studies have focused on the NP export and detoxification processes in cells. The complete process of NP uptake, distribution, transformation, and exocytosis from the cell remains unknown. Furthermore, dissolved ions from metal and metal oxide NPs may also cause cytotoxicity and complicate mechanistic investigations. In fact, the contribution of dissolved ions to the overall toxicity of mammalian cells caused by NP exposure is still largely unclear. Metal ions released from NPs are typically isolated by centrifugation.[15] However, the standard centrifugation protocols will be inadequate for the separation of NPs and the complex cell medium. Thus, centrifugal ultrafiltration tubes were employed in this study to quantify the contribution of dissolved ions to the total NP cytotoxicity.

In this study, we focused on the cytotoxicity of CuO NPs. Recent studies have shown that CuO NPs display significant toxicity to algae,[16] bacteria,[17] and fish.[18] For human cells, Karlsson et al. reported that CuO NPs were significantly more toxic than ZnO, Fe_2O_3, and TiO_2 NPs, and CuO NPs resulted in oxidative stress and DNA damage of human cells.[19] However, they did not study the time sequence between DNA damage and oxidative stress. In addition, they did not examine how NPs affect gene expression. Therefore, in this work, we mainly focused on the relationship between reactive

Received: May 8, 2012
Published: June 11, 2012

oxygen species (ROS) generation and DNA damage and gene expression during CuO NPs exposure. Moreover, the dissolved Cu^{2+} from CuO NPs may also induce cellular damage such as oxidative damage and DNA damage, and the contribution of these dissolved Cu^{2+} needs further evaluation. Human lung epithelial cells (line A549) were chosen as the test cell line in this study because it is a representative target cell commonly employed in many pulmonary toxicological studies.[20−22] Therefore, the goal of this study was to investigate (1) the mechanism of CuO NP cytotoxicity to the human lung epithelial cells (A549 cell line) through the determination of ROS production and DNA damage over time and (2) the uptake and export processes for CuO NPs. In addition, the dissolved Cu ion concentration from CuO NPs in the cell medium was directly measured using centrifugal ultrafiltration tubes, and the ion contribution to the overall CuO NP toxicity was determined. The findings of this study will provide insight into the risk of CuO NP exposure to humans and the potential need for modified NPs handling protocols and regulatory guidance.

MATERIALS AND METHODS

Cell Culture and NPs Suspension Characterization. The A549 cell line was purchased from Shanghai Institute for Biological Sciences, Chinese Academy of Science. Cells were cultured in nutrient mixture F12 Ham Kaighn's modified medium (F12K, Sigma-Aldrich, St. Louis, MO) supplemented with 10% fetal bovine serum (FBS, PAA Laboratories GmbH, Austria), 2 mM L-glutamine (Amresco Inc., United States), and 1% penicillin streptomycin (Tian Jin Hao Yang Biological Manufacture Co., LTE) (F12K-FBS medium) (Table S1 in the Supporting Information). Cells were maintained at 37 °C in an incubator with 5% CO_2.

CuO NPs and CuO bulk particles (BPs) were purchased from Beijing Nachen S&T Ltd., and the characterization of CuO NPs is shown in Figure S1 and Table S2 in the Supporting Information. A stock solution of CuO NPs (1000 mg/L) was prepared in the F12K-FBS medium and sonicated for 10 min before aseptic addition to the tissue culture plates. The number of cells added in each well was identical (5×10^3 cells/well). Then, different volumes of CuO NPs stock solution were added to the cell cultures to achieve predetermined concentrations of CuO NPs (5 and 15 mg/L) for cell incubation. The hydrodynamic diameter and ζ-potential of CuO NPs at 5 and 15 mg/L in the F12K-FBS and ultrapure water were determined using a Nanosizer (Nano S90, Malvern Instruments Ltd., United Kingdom). The particle size of CuO NPs was also evaluated by a transmission electron microscopy (TEM, JEM-2100, JEOL, Japan).[18]

Cell Viability Assay. Cell viability was determined by Cell Counting Kit-8 (Beyotime Institute of Biotechnology).[23] Briefly, 5×10^3 cells were spread onto each 96-multiwell plate. Cells in each well were treated with different concentrations of CuO NPs or BPs (0.5, 1, 5, 20, 30, 40, 50, and 100 mg/L) at 37 °C for 6, 12, 24, and 48 h. The cells were then incubated with 10 μL of cholecystokinin octapeptide (CCK-8) for 4 h, and the absorbance was measured at 450 nm. The mean absorbance of nonexposed cells served as the reference value for calculating percentage of cellular viability. Finally, the half maximal inhibitory concentration (IC_{50}) was calculated according to cell viability from various CuO NP exposures.

CuO NPs Dissolution and Cu^{2+} Solution Preparation. The free Cu^{2+} ion concentration dissolved from CuO NPs into the cell medium was determined using a modified procedure by Navarro et al.[24] The CuO NPs (15 mg/L) in the F12K-FBS medium were allowed to equilibrate for 1, 2, 3, 4, and 5 days (5% CO_2, 37 °C). CuO NP suspensions were then centrifuged for 30 min at 1500g using ultrafiltrate centrifugal tubes (3 kDa, Millipore). The Cu concentration in the filtrate was determined using flame atomic absorption spectrometry (FAAS, Thermo SOLAAR M6, United States).

Different concentrations of Cu^{2+} (0, 0.5, 1, 2, 3, 4, 6, 8, and 10 mg/L) using $CuSO_4{\cdot}5H_2O$ were added to F12K-FBS medium at 37 °C for 24 h. These solutions were centrifuged using ultrafiltrate centrifugal tubes (1500g, 30 min), and the Cu concentration was determined using FAAS. The concentration of Cu^{2+} solution used in the following cell tests was based on the measured free Cu ion concentration dissolved from CuO NPs. The total Cu^{2+} concentration (including the free and bound Cu^{2+}) dissolved from CuO NPs was also determined. Briefly, 15 mg/L CuO NPs was centrifuged at 9390g for 30 min after equilibration for 24 h, and the supernatant was analyzed by FAAS.

TEM Observation and Endocytosis Inhibition. The distribution and location of CuO NPs in cells were observed using TEM[9] operated at an accelerating voltage of 80 kV and further analyzed by the energy dispersive spectroscopy (EDS) (INCA100, Oxfordshire, United Kingdom). Briefly, the treated cells by CuO NPs (15 mg/L) and Cu^{2+} (2.5 mg/L) were trypsinized and washed 3−4 times in phosphate buffer solution (PBS) and fixed in 2.5% glutaraldehyde for 1 h. The fixed cells were postfixed in 1% osmium tetroxide for 1 h and dehydrated in a graded series of ethanol (50, 70, 80, 95, and 100%, each for 10 min at room temperature). After dehydration, the samples were incubated overnight in a mixture of ethanol and Araldite CY212 resin (1:1, v/v). The specimens were embedded in pure resin for 48 h at 60 °C. The polymerized block was then cut into 60 nm thick sections that were mounted on nickel grids. The CuO NPs in the cells were observed using TEM operated at an accelerating voltage of 80 kV and further analyzed by EDS. After they were treated with 15 mg/L CuO NPs for 12 h, A549 cells (1×10^6 cells/mL before treatment) were collected and washed with 0.02 M EDTA for 30 s and three times with PBS[14,25] to remove the adsorbed NPs on the cell membrane. Then, the nuclei of the washed A549 cells were isolated using the method of Fisher and Harris.[26] The number of nuclei was counted, and the nuclei were also digested for Cu content determination using graphite furnace-atomic absorption spectrometry (GAAS).

A549 cells (1×10^6 cells/mL) were incubated with endocytosis inhibitors (10 mM NaN_3 and 50 mM 2-deoxyglucose) for 30 min[13] and then treated with 5 and 15 mg/L CuO NPs and 2.5 mg/L Cu^{2+}, respectively, for another 12 h. The CuO NPs and Cu^{2+} treatments without NaN_3 and 2-deoxyglucose were used as controls. After incubation, the cells were collected, treated with 0.02 M EDTA for 30 s,[27] and washed three times with PBS[14] to remove the adsorbed NPs on the cell membrane. After centrifugation (1500g, 10 min), the A549 cells were collected, and the cell number was counted. The cells were then digested, and the Cu contents were determined by GAAS.

Reactive Oxygen Species, Mitochondrial Membrane Potential, and Lysosomal Staining. 2,7-Dichlorodihydrofluorescein diacetate (DCF-DA, Beyotime Institute of Biotechnology) is non-fluorescent unless oxidized by the intracellular ROS.[9] Time-dependent measurements of the generation of ROS were conducted by incubating 1×10^6 cells with CuO NPs (5 and 15 mg/L) and Cu^{2+} (2.5 mg/L) for 0.5, 1, 2, 3, 4, 8, 16, and 24 h, followed by staining with DCF-DA for 30 min at 37 °C. Cells were then washed twice in serum-free medium and analyzed using a flow cytometer (Becton Dickinson, Mountain View, United States) at an excitation wavelength of 488 nm and emission wavelengths of 530 and 610 nm for DCF-DA. The detection of ROS was expressed as: relative ROS sensor level (%) = mean DCF fluorescence intensity (FI) [NP- and Cu^{2+}-treated] × 100/mean DCF FI [control].

Mitochondrial membrane potentials (MMP, $\Delta\Psi$m) of CuO NPs and Cu^{2+}-treated cells were measured using flow cytometry. A549 cells (1×10^5 cells/mL) were plated and treated with 5 mg/L CuO NPs, 15 mg/L CuO NPs, or 2.5 mg/L Cu^{2+} ions for 2, 4, 8, 16, and 24 h at 37 °C. The fluorescent probe 5,5′,6,6′-tetrachloro-1,1′,3,3′-tetraethylimidacarbocyanine iodide (JC-1, 5 μM) was diluted in F12K medium before addition to cells. Flow cytometry analysis was performed using a FACScan or LSR (Becton Dickinson) equipped with a single 488 nm argon laser. JC-1 was analyzed in both FL-1 channel and FL-2 channel.[27] The MMP change was expressed as: mitochondrial depolarization level (% of control) = ratio of mean green (FL-2) and mean red (FL-1) [NP- and Cu^{2+}-treated] × 100/ratio of mean green (FL-2) and mean red (FL-1) [control].

Lysosomes were stained and observed by a confocal microscope (Olympus Confocal 1P/FCS).[14] After treatment of the cells with CuO NPs (5 and 15 mg/L) and Cu^{2+} (2.5 mg/L) for 24 h, the cells were washed and incubated for 30 min with 35 nM Lyso-Tracker Red (Beyotime Institute of Biotechnology). The cell culture plates were visualized with confocal microscope. Images were processed using Olympus Confocal Software.[13] The number of successfully stained cells was determined as: lysosomal stained cells (%) = number of lysosomal stained cells × 100/total number of cells from each treatment.

Real-Time Polymerase Chain Reaction (RT-PCR) and Comet Assay. After treated with CuO NPs, total RNA in A549 cells was extracted using Trizol Plus RNA purification kit (Invitrogen).[28] RT-PCR was performed with a Takara SYBR Premix DimerEraserTM (Perfect Real Time). The primers for human *p38* and *p53* were designed according to Primer select software. The human sequences for the primers are as follows: (1) *β*-actin forward, CCCCCATGCCATCCTGCGTCTG, and reverse, CTCGGCCGTGGTGGTGAAGC; (2) p38 forward, CAGGGCTCCAGAAATTATGTTGAA, and reverse, CTGGAAAGATGGGCCTGTTAGAAA; (3) p53 forward, GACCGGCGCACAGAGGAAGAGAAT, and reverse, TGGGGAGAGGAGCTGGTGTTGTTG. The final PCR mixture contained 1 *μ*L of cDNA template and 400 nmol/L of the forward and reverse primers in a final volume of 20 *μ*L. Samples were run concurrently with a standard curve prepared from the PCR products. PCR conditions were three steps of 94 °C for 30 s and 40 cycles of 94 °C for 15 s and 60 °C, and 72 °C for 30 s, respectively. A melting curve analysis was used to confirm specific replicon formation. Expression levels were determined from cycle thresholds using a standard curve, normalized to human *β*-actin expression levels, and were expressed as relative expression amounts as compared with the control using an equation: relative expression amount of target gene = $2^{-\Delta\Delta Ct}$, where $\Delta\Delta Ct = (Ct_{gene,treatment} - Ct_{actin,treatment}) - (Ct_{gene,control} - Ct_{actin,control})$.[29] In addition, DNA damage in A549 cells was examined using a modified alkaline single-cell gel electrophoresis (Comet assay)[30] and subsequent staining in ethidium bromide (EB). Treated cells were embedded in 0.6% low melting agarose (Pronadisa, Spain) on Comet slides (Trevigen, Gaithersburg, MD) and lysed in prechilled lysis solution (2.5 M NaCl, 0.1 M EDTA, and 10 mM Tris base, pH 10) with 1% Triton X (Trevigen, Gaithersburg, MD) for 2 h at 4 °C. Cells were then subjected to denaturation in alkaline buffer (0.3 M NaCl and 1 mM EDTA) for 20 min in dark at room temperature. Electrophoresis was performed at 25 V and 300 mA for 40 min. The slides were immersed in neutralization buffer (0.5 M Tris-HCl, pH 7.5) for 15 min. The slides were air-dried and stained with EB. The tail moments of the cell nucleus were measured as a function of DNA damage. Analysis was done using CASP software 1.2.3, and 50 Comets were analyzed for per exposure concentration

Lactase Dehydrogenase (LDH) Release Assay. LDH leakage can be measured as an indicator of cell membrane integrity in cultured cells. We measured LDH activity using a cytotoxicity detection kit (Nanjing Jiancheng Co., China).[31] A549 cells (1×10^5 cells/mL) were treated by CuO NPs (5 and 15 mg/L) and Cu^{2+} ions (2.5 mg/L) for 4 and 24 h, and then, 20 *μ*L of the supernatant was transferred to another plate that was subsequently amended with 25 *μ*L of substrate buffer solution and 5 *μ*L of coenzyme. The plate was incubated (37 °C, 5% CO_2) for 15 min, followed by the addition of 25 *μ*L of 2,4-dinitrophenylhydrazine for another 15 min. Finally, a termination agent (0.4 mol/L NaOH, 250 *μ*L) was added to each well for 5 min at room temperature. The absorbance was recorded at 450 nm using a Multiskan Spectrum (Thermo Electron Co., Finland).

CuO NPs and Cu ion Export Study. The NP export studies followed the method of Jiang et al.[14] A549 cells (1×10^5 cells/mL) were plated and incubated with CuO NPs (5 and 15 mg/L) and Cu^{2+} (2.5 mg/L) for 24 h to achieve particle and ion uptake. The cells were then treated with 0.02 M EDTA for 30 s to remove the adsorbed Cu^{2+} on the cell membrane.[25] The cells were then washed three times with PBS to remove the adsorbed CuO NPs on the membrane[14] and were supplied with fresh F12K-FBS medium.

NP exocytosis from the cells was quantified by determining the total Cu concentration of the fresh cell medium after different exposure times (2, 4, 6, 8, 10, 12, 16, 20, and 24 h) using FAAS.[32] Cell viability was also evaluated after with the addition of fresh cell medium. To evaluate the kinetics of NP excretion, the A549 cells (1×10^5 cells/mL) were incubated with CuO NPs (5, 15 mg/L) and Cu^{2+} (2.5 mg/L) for 24 h. The cells were then treated with 0.02 M EDTA for 30 s and washed three times with PBS, and fresh medium was then added to different samples at 2 h intervals. The Cu in the replenished solution was determined by AAS.

RESULTS AND DISCUSSION

Cell Viability. CuO NPs at low concentrations (0.5 and 1 mg/L) had insignificant toxicity to A549 cells and, in fact, demonstrated growth promotion (Figure 1A), which is likely

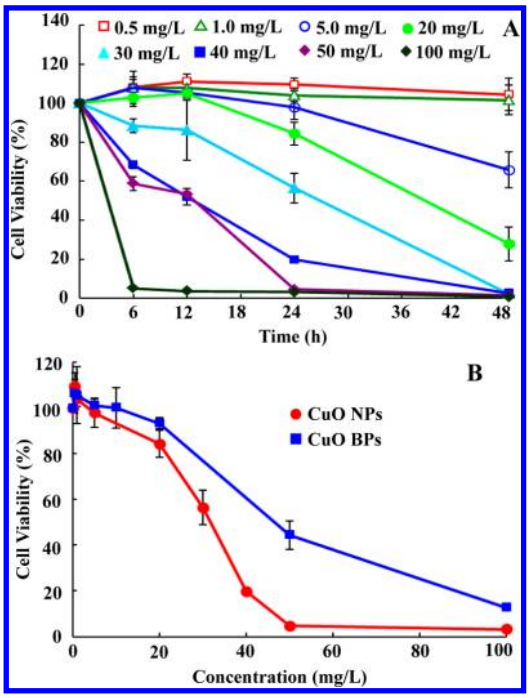

Figure 1. A549 cell viability measured with the CCK-8 assay after exposure to different conditions: (A) cell viability after exposure to 0–100 mg/L CuO NPs for 6, 12, 24, and 48 h and (B) cell viability after 24 h of exposure to CuO NPs and BPs at different concentrations. Data are showed as mean values ± standard deviations, $n = 5$.

the result of Cu being a required micronutrient. The toxicity of CuO NPs at moderate concentrations (20 and 30 mg/L) began to appear after exposure for 12 h and became significantly greater in the subsequent 24 h. For high concentrations of CuO NPs (40, 50, and 100 mg/L), toxicity to A549 cells was the greatest at 24 h, and then, cell viability dropped to 2.62, 0.42, and 0.7% of control for the remainder of the assay, respectively. The toxicity of CuO NPs was concentration-dependent (Figure 1B), and the 24 h IC_{50} was calculated as 15 mg/L. Thus, 15 mg/L was chosen in the following toxicity studies, and 5 mg/L was also examined for comparison. The 24 h IC_{50} values of cylinder Si,[33] chitosan,[34] and Si-coated magnetic[35] NPs to A549 cells were reported in the range of 141 ± 5, 1100–1200, and 4000 mg/L, respectively. Thus, CuO NPs had a much higher toxicity potential, a finding supported by Karlsson et al.,[19] who observed that CuO NPs were more toxic to A549 cells than ZnO and TiO_2 NPs. The average particle size of CuO NPs was observed as 20–40 nm by TEM imaging (Figure S1 in the

dx.doi.org/10.1021/tx3002093 | Chem. Res. Toxicol. 2012, 25, 1512–1521

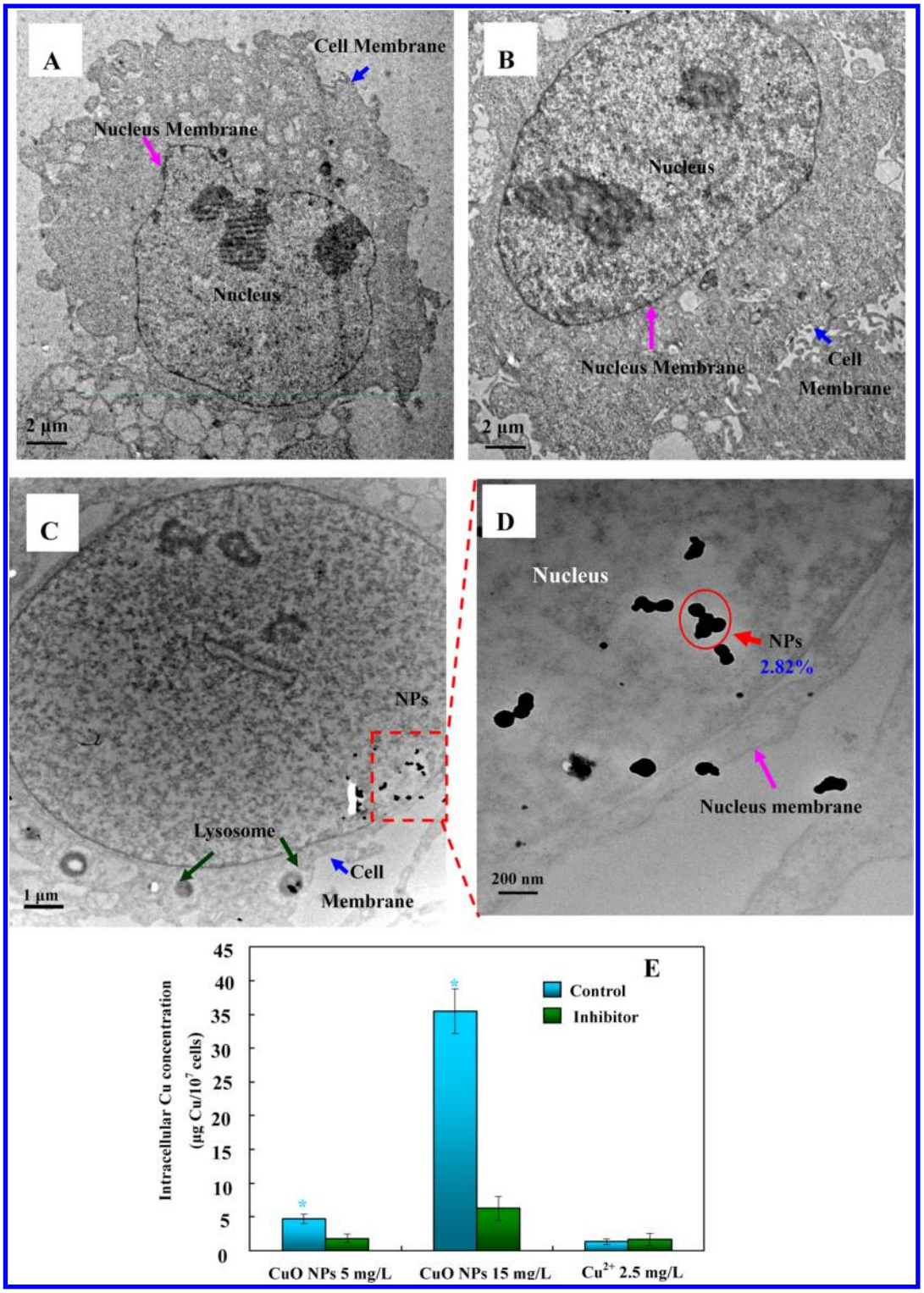

Figure 2. TEM observations of A549 cells after exposure to CuO NPs (15 mg/L) or Cu^{2+} (2.5 mg/L) for 12 h. (A) Control, (B) treated by 2.5 mg/L Cu^{2+}, (C) treated by 15 mg/L CuO NPs, and (D) an enlarged image of NPs in the nucleus from the red frame in image C. The NPs-accumulated points are shown by a red arrow and were analyzed by EDS. The Cu atomic percent of each point is shown in blue color. (E) Inhibition of endocytosis. A549 cells were pretreated for 30 min with endocytosis inhibitors (10 mM NaN_3, 50 mM 2-deoxyglucose), followed by exposure to 5 or 15 mg/L CuO NPs or 2.5 mg/L Cu^{2+} for 12 h at 37 °C with 5% CO_2. Error bars represent the standard deviation of the mean concentration for at least three replicate measurements. The intracellular Cu concentration of CuO NPs (5 and 15 mg/L) and Cu^{2+} (2.5 mg/L) in the presence of NaN_3 and 2-deoxyglucose was compared with the control group in the absence of endocytosis inhibitors ($p < 0.05$).

Supporting Information), smaller than that of Si (214 ± 29 nm), chitosan (>109 nm), and Si-coated magnetic NPs (50 nm), which may partly explain the higher toxicity of CuO NPs. CuO NPs in the cell medium were able to release large quantities of metal ions, which could be another reason for higher toxicity to A549 cells.[17]

dx.doi.org/10.1021/tx3002093 | Chem. Res. Toxicol. 2012, 25, 1512−1521

CuO BPs toxicity to A549 cells was also examined at 0−100 mg/L for 24 h (Figure 1B). Similar to CuO NPs, cell viabilities upon CuO BP exposure were concentration dependent. The 24 h IC_{50} (58 mg/L) was more than three times higher than 24 h IC_{50} of CuO NPs, clearly showing that CuO NPs have greater toxicity, which agrees with previous studies.[18,36] Because of the higher potential toxicity of CuO NPs to A549 cells, the metal oxide NP was to focus of our subsequent mechanistic studies.

CuO NPs Dissolution in Cell Culture Medium. Centrifugation methods are typically used to remove NPs for determination of the extent of metal and metal oxide NP dissolution.[15] This method was also used to examine the Cu concentration dissolved from CuO NPs in the cell medium, 8.44 mg/L. However, after high-speed centrifugation (9391*g*), CuO NPs still remained in the medium as determined by optical microscopic observation, largely due to small NP size and their stability in the cell medium (Figure S2A in the Supporting Information). Similar results are also reported in ZnO NPs dissolution studies; centrifugation (22000*g*) of ZnO NPs suspensions for 20 min was unable to completely remove ZnO from DMEM medium.[5] Therefore, another Cu^{2+} ion separation method using centrifugal ultrafiltration tubes[24] was employed in this study. The centrifugal ultrafiltration tubes (nominal molecular weight cutoff, 3 kDa) can separate most of proteins (about 98% in Table S3 in the Supporting Information) from the filtrate. Because the F12K-FBS contained many macromolecular proteins, CuO NPs in amino acid/protein-rich medium could generate Cu^{2+}-peptide/protein complexes, rather than dissociated Cu^{2+}. Thus, the determined Cu^{2+} concentration would be free Cu^{2+} because the CuO NPs and protein-bound Cu^{2+} were separated from the filtrate. The dissolution of CuO NPs did not reach equilibrium after 5 days (37 °C, 5% CO_2) (Figure S2B in the Supporting Information), and the dissolved free Cu concentration was 1.08 mg/L after 24 h of dissolution. Notably, Gunawan et al.[17] reported that copper−peptide complexes (bound Cu^{2+}) are less cytotoxic as compared to uncoordinated copper ions formed by the addition of copper salts (free Cu^{2+}).

To examine the contribution of dissolved Cu^{2+} to CuO NPs toxicity, a dissolved Cu^{2+} treatment supplied by copper salts is needed.[17] The relationship between Cu^{2+} concentration (supplied by $CuSO_4{\cdot}5H_2O$) before complexation with proteins in the medium and the free Cu^{2+} concentration after complexation was studied (Figure S2C in the Supporting Information). The experimental values were well described by a quadratic model (R^2 = 0.997). The added Cu^{2+} concentration (2.43 mg/L) was calculated according to the quadratic model fitting results when the concentration of free Cu^{2+} released from CuO NPs reached 1.08 mg/L after 24 h of dissolution. Therefore, the Cu^{2+} toxicity to A549 cells in following studies was evaluated by exposing the cells in 2.5 mg/L Cu^{2+} (higher than the calculated total Cu^{2+} concentration). Our previous study reported CuO NPs dissolution with an equilibrium concentration of Cu^{2+} at 10 μg/L in BG11 medium.[16] Clearly, CuO NPs had a high solubility in the cell medium, indicating that Cu^{2+} and Cu^{2+}-peptide/protein complexes could contribute to a higher toxicity to A549 cells than observed for algae. The main reasons for the high Cu^{2+} solubility were (a) that CuO NP interactions with amino acid/protein or inorganic constituents could result in further Cu^{2+} dissolution from metal oxide NPs and (b) that CO_2 presented in the incubator (5%) and medium could increase the dissolution of CuO NPs.[37] Indeed, the content of H^+, HCO_3^-, and CO_2 for cell culture was quite close to the bloodstream environment in humans and animals.[38] Thus, when CuO NPs entered the pulmonary bloodstream, they may quickly dissolve and exhibit Cu^{2+} toxicity to lung tissues.

CuO NPs Uptake and Distribution in A549 Cells. TEM was employed to investigate the distribution of intracellular CuO NPs. There were no visible abnormalities in the normal cells of the control and 2.5 mg/L Cu^{2+} treated cells after 12 h (Figure 2A,B), and the nucleoplasm was surrounded by the complete nuclear membrane (Figure S3A,C in the Supporting Information). After incubation with 15 mg/L CuO NPs for 12 h, CuO NPs were observed in subcellular structures including the cytoplasm, endosomes/lysosomes, and mitochondria (Figure S3E,F,J,K in the Supporting Information). To confirm the presence of Cu in these structures (Figure 2C,D), the electron diffraction pattern of CuO NPs was obtained (Figure S4 in the Supporting Information) and confirmed that the intracellular NPs are indeed CuO. Additionally, it has been reported in the literature that accumulation of excess proteins in lysosomes could cause accumulation of secondary lysosomes.[39] In our study, several secondary lysosomes in A549 cell were observed after 12 h of CuO NPs exposure (Figure S3I in the Supporting Information), while there were few secondary lysosomes in the control. This result suggests that the number of secondary lysosomes may increase upon NP entry into the lysosomes. Additionally, CuO NPs were observed in primary and secondary lysosome in the cytoplasm of the cells (Figure S3J,K in the Supporting Information), suggesting that particle entry into the cells is through endocytosis rather than diffusion. To further explore the effect of CuO NPs on lysosomes, we measured organelle activity by confocal laser scanning microscopy (Figure S5 in the Supporting Information). The activity of lysosomes in cells treated with 15 mg/L CuO NPs was significantly lower than the control. This suggests that CuO NPs inhibit lysosomal activity, observations supported by the findings of Wang et al.[23] Damage to lysosomal membranes may lead to subsequent translocation of the CuO NPs to other organelles such as mitochondria and the nucleus.

CuO NPs were observed in the nucleus by TEM observation (Figure 2C,D), and the Cu content in the cell nuclei was quantified as 6.59 ± 1.21 μg/10^7 nuclei (Figure S6 in the Supporting Information). Intracellular CuO NPs were approximately 40 nm, and some significantly larger CuO NPs aggregates were evident (Figure 2D). The TEM-determined particle size of CuO NPs was between 20 and 40 nm (Figure S1 in the Supporting Information), but the hydrodynamic diameter of CuO NPs in the cell medium was 185 nm (Table S4 in the Supporting Information), clearly showing CuO NP aggregation. Previous studies have shown that macromolecules cannot access the nucleus from cytoplasm by endocytosis (e.g., proteins and viral genome) but can go through the nuclear pore complexes (NPCs)[40] or destroy the nuclear membranes (e.g., multiwalled carbon nanotubes).[41] The diameter of the central pore of the NPC, as measured by electron microscopy, was 44 nm in *Xenopus* oocytes.[42] Another study reported that the size of the central pore of the NPC in vertebrate cells was approximately 50 nm.[43] Thus, the individual CuO NPs smaller than 50 nm may be able to enter the nucleus via nuclear pore, and some of the individual CuO NPs may aggregate together in the nucleus as shown in Figure 2D. The individual CuO NPs in the nucleus may, on the other hand; as shown in Figure 2C,D, the nuclear membrane

was not complete after 12 h of exposure of 15 mg/L CuO NPs. Thus, CuO NPs of larger size, as well as CuO NP aggregates, may enter the cell nucleus by direct physical injury of nucleus membrane. The CuO NPs inside the nucleus may be able to damage DNA directly. Physical DNA damage by other NPs (e.g., C_{60}) was reported by previous studies.[44,45]

To further investigate the pathway of CuO NP uptake, we performed a series of experiments with the endocytic inhibitor (Figure 2E). For the Cu^{2+} ion (2.5 mg/L) treatments, the intracellular Cu contents were lower, and there was no difference between the cells with and without NaN_3 and 2-deoxyglucose pretreatment. For the CuO NP (5 and 15 mg/L) treatments, intracellular Cu contents significantly decreased (more than 50%) upon pretreatment with NaN_3 and 2-deoxyglucose, clearly suggesting that endocytosis was a major pathway of NPs uptake in A549 cells. Similarly, Asati et al.[13] and Jiang et al.[14] both focused on endocytosis as the primary uptake pathway for CeO_2 and zwitterionic quantum Dot NPs. To evaluate the effects of short- and long-term CuO exposure on the cell membrane integrity, LDH release from A549 cells was determined after 4 and 24 h exposures (Figure S7 in the Supporting Information). After 4 h of exposure to CuO NPs (5 and 15 mg/L) and Cu^{2+} (2.5 mg/L), LDH release from A549 cells did not significantly increase. This suggests that NP uptake did not cause damage to phospholipid bilayer as would be expected from direct penetration, further implicating endocytosis as the primary accumulation mechanism. In contrast, Cu^{2+} can efficiently pass through the cell membrane via copper transport proteins and thereby did not damage the membrane.[46] Conversely, after 24 h of exposure, 15 mg/L CuO NPs induced significantly higher LDH release (192% of control) from A549 cells ($p < 0.05$), while 5 mg/L CuO NPs and 2.5 mg/L Cu^{2+} induced slight LDH leakage (Figure S7 in the Supporting Information).

ROS Generation and Mitochondrial Depolarization. After 2 h of exposure, the ROS levels in all Cu treatments were much higher than unexposed controls; the 5 mg/L CuO NPs, 15 mg/L CuO NPs, and 2.5 mg/L Cu^{2+} treatments were 208, 380, and 233% significantly greater than the controls, respectively ($p < 0.05$) (Figure 3A). A549 cells treated by Cu^{2+} ions exhibited a higher ROS level than the control cells, although the intracellular Cu was low (Figure 2E). By 4 h, the ROS levels had decreased and leveled off to near the controls. For 15 mg/L CuO NPs and 2.5 mg/L Cu^{2+} ions, the ROS levels were significantly increased at 16 h ($p < 0.05$). The initial oxidative stress upon Cu exposure interaction with the cells (2 h, Figure 3A) gradually abated in response to the antioxidant defense system of cells (4–8 h, Figure 3A). During longer exposures, depletion of antioxidant enzymes such as GPx, catalase, and SOD[30] is possible, with ROS accumulation potentially increasing again ($p < 0.05$).

TEM analysis showed that CuO NPs could interact with mitochondria (Figure S3F in the Supporting Information), potentially impacting organelle function. The mitochondrial depolarization level was determined by measuring the MMP using flow cytometer (Figure 3B). CuO NPs at 15 mg/L effectively decreased MMP of A549 cells relative to other treatments at all exposure times. The trend of mitochondrial depolarization level from 2 to 24 h was similar to ROS production level (Figure 3B), suggesting that CuO NP-induced mitochondrial depolarization may be mediated by ROS generation. Levraut et al. observed that ROS generated from

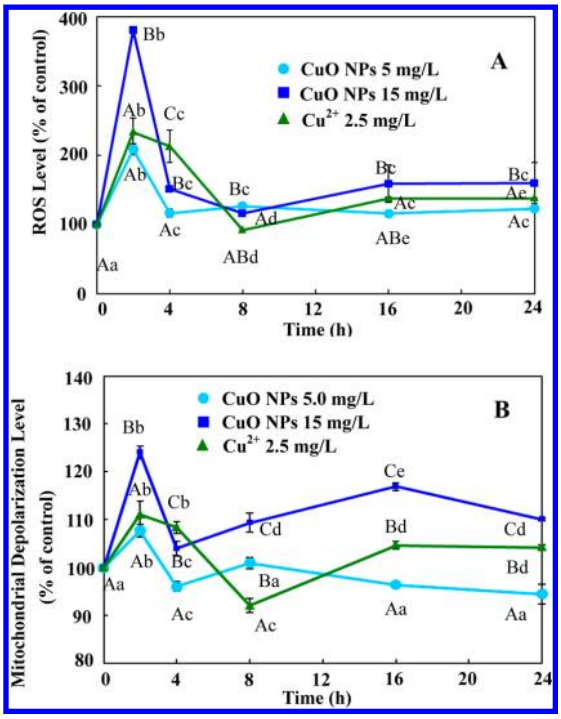

Figure 3. (A) Assessment of ROS generation by A549 after exposure to CuO NPs (5 and 15 mg/L) and Cu^{2+} (2.5 mg/L) for 2, 4, 8, 16, and 24 h. Treated cells were incubated with DCF-DA dyes for 30 min and analyzed with a LSR flow cytometer. The FI comparison indicated the formation of ROS. The calculation is described as follows: relative ROS sensor level (%) = mean DCF FI [treated]/mean DCF FI [control] × 100. (B) Assessment of mitochondrial depolarization by measuring the MMP ($\Delta\Psi m$) using JC-1 fluorescent dyes. Flow cytometric analysis was performed after the addition of the CuO NPs (5 or 15 mg/L) or Cu^{2+} (2.5 mg/L) for 2, 4, 8, 16, and 24 h. A decrease in MMP could lead to mitochondrial depolarization. For a fixed treatment (5 mg/L CuO NPs, 15 mg/L CuO NPs, or 2.5 mg/L Cu^{2+}), points followed by different letters (a–e) indicate significant differences at different exposure times ($p < 0.05$). Points followed by letters A–C indicate significant differences among different treatments (5 mg/L CuO NPs, 15 mg/L CuO NPs, or 2.5 mg/L Cu^{2+}) at a fixed exposure time (0, 2, 4, 8, 16, or 24 h) ($p < 0.05$).

the mitochondrial electron transport chain could contribute to the observed membrane depolarization.[47]

These data suggest that CuO NPs were located in the mitochondria of A549 cells after 2 h of CuO NPs treatment, subsequently altering mitochondrial structures, disrupting the electron transport chain, and increasing cytoplasmic ROS production.[23] Similarly, ZnO NPs were capable of robust spontaneous ROS generation to RAW 264.7 cells after 1 h of exposure.[5] However, Eom and Choi[10] reported that Jurkat cells showed low levels of ROS in response to 5–30 min Ag NP exposure. The authors noted that ROS was significantly generated from the cells only after 24 h of exposure, suggesting different susceptibilities of Jurkat and A549 cells. Wang et al.[23] showed that cytotoxicity from Au nanorods (NRs) varied significantly with cell type in in vitro studies. Specifically, it was reported that Au NRs could induce mitochondrial damage of A549 cells, while Au NRs did not decrease the MMP and destroy mitochondrial structures in normal bronchial epithelial cells and primary adult stem cells. ROS were generated mainly in the mitochondria of the cell[9] where organelle function was destroyed.

dx.doi.org/10.1021/tx3002093 | Chem. Res. Toxicol. 2012, 25, 1512–1521

Gene Expression and DNA Damage. Previous studies reported that there was a close relationship between *p38*/*p53* activation and DNA damage,[48,49] which makes *p38* and *p53* sensitive molecular biomarkers to assess genotoxicity of CuO NPs. Therefore, the responding signal transduction pathway of DNA damage was investigated by examining *p38* and *p53* response (Figure 4A,B). A temporal gene expression analysis revealed that expression of *p38* and *p53* increased as early as 4 h after exposure to 15 mg/L CuO NPs, while expression of *p38* and *p53* was unchanged after exposure of 2.5 mg/L Cu^{2+}. Given the activation of *p38* and *p53*, CuO NPs may result in cell cycle arrest[10] and even cell apoptosis.[10,28] Further analysis using the Comet assay detected a combination of single-strand breaks, double-strand breaks, and alkaline labile sites (Figure 4C). The Comet assay revealed that a time-dependent increase in tail moment as compared to control after exposure to CuO NPs but to a lesser extent for the exposure to Cu^{2+}. The tail moment began to show a significant increase after exposure to 15 mg/L CuO NPs (450% of control) for 8 h. The tail moment dramatically increased with increasing exposure time and reached a maximum value (460% of control) after 24 h of exposure to NPs. Conversely, the tail moment increased significantly only at 24 h of exposure to 5 mg/L CuO NPs (130% of control) and 2.5 mg/L Cu^{2+} (125% of control), suggesting that the DNA damage was a cumulative process in A549 cells. Interestingly, DNA damage from CuO BPs at levels up to 50 mg/L was much lower than that of CuO NPs at 15 mg/L (Figure S8 in the Supporting Information), which agrees with the cell viability results (Figure 1B).

Previous studies speculated that DNA damage in NP-exposed cells was induced by oxidative stress and suggest that ROS generation and oxidative stress in the cell may cause subsequent oxidative damage to DNA through free radical attack.[7,9] However, until now, nothing has been known about the time sequence of ROS production and DNA damage. From our data, it is clear that the DNA damage caused by CuO NPs results from oxidative stress after 2 h of exposure, followed by activation *p38* and *p53* at 4 h, finally causing irreversible DNA damage after 8 h.

NPs and Cu Ion Exclusion. The export kinetics of Cu from A549 cells was examined after pretreating cells with CuO NPs (5 and 15 mg/L) and Cu^{2+} (2.5 mg/L) (Figure 5A). For CuO NPs-treated cells, the exported Cu concentration generally increased with increasing exposure time (12−24 h), while the Cu exclusion from Cu^{2+} pretreated cells showed strong fluctuation over time. Cu export concentrations from cells were time-dependent for all treatments (Figure 5B). After 24 h of export, the removal process reached near equilibrium, and the total excreted Cu contents were 0.8, 0.9, and 0.06 mg/L for 5 and 15 mg/L CuO NPs and 2.5 mg/L Cu^{2+} treatments, respectively. These findings only partially agree with Jiang et al.,[14] who observed that half of the NPs (zwitterionic Quantum Dot) were quickly removed by live HeLa cells. The authors showed that the internalized DPA-QDs were stored in lysosomes, and delivery of the NP-containing vesicles back to the cell periphery for export was highly efficient. In contrast, others have reported that Au NPs in A549 cells were more difficult to export because of particle translocation from lysosomes to mitochondria, which caused cytotoxicity.[23] It is likely in our study that a fraction of CuO NPs were not excreted by A549 cells because of the particle deposition in the mitochondria and nucleus as described above. After exposure to CuO NPs (15 mg/L) for 24 h and export for another 24 h,

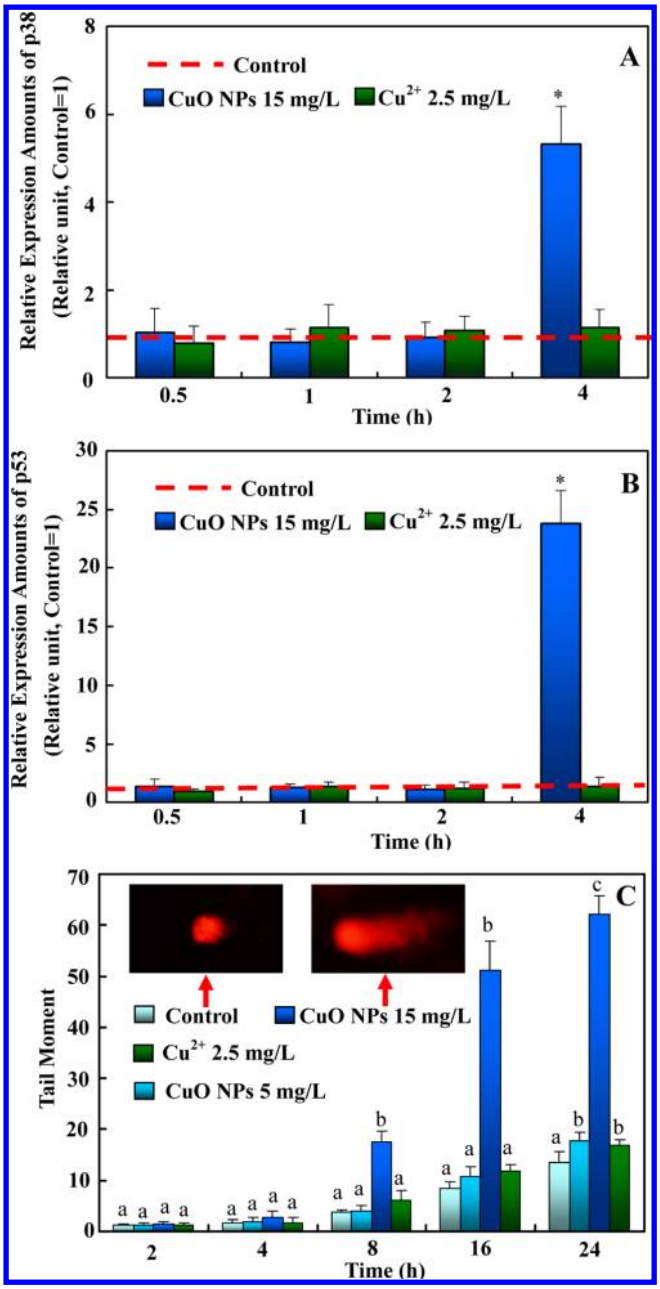

Figure 4. Relative expression amounts of *p38*/*p53* and DNA damage (Comet assay) in A549 cells exposed to CuO NPs and Cu^{2+} ions. The relative expression amounts of *p38* (A) and *p53* (B) after exposure to 15 mg/L CuO NPs and 2.5 mg/L Cu^{2+} ions for 0.5, 1, 2, and 4 h. The expressions of *p38* and *p53* were measured in the nuclear fractions. The densitometric values for the expressions of the proteins were normalized to those of actin and presented as relative units as compared to the control using an equation: relative expression amount of target gene = $2^{-\Delta\Delta Ct}$, where $\Delta\Delta Ct = (Ct_{gene,treatment} - Ct_{actin,treatment}) - (Ct_{gene,control} - Ct_{actin,control})$. Data represent mean values ± standard deviations (n = 3). The asterisk indicates the significant difference between control and other treatments by using ANOVA ($p < 0.05$). For the Comet assay (C), the tail moments values of DNA were obtained by analyzing 50 random comet images from each treatment. Bars followed by different letters (a−c) indicate significant differences among different treatments (5 mg/L CuO NPs, 15 mg/L CuO NPs, or 2.5 mg/L Cu^{2+}) in a fixed exposure time (2, 4, 8, 16, and 24 h) ($p < 0.05$). Inserts of panel C are Comet images of untreated and 15 mg/L CuO NPs treated cells, respectively.

dx.doi.org/10.1021/tx3002093 | Chem. Res. Toxicol. 2012, 25, 1512−1521

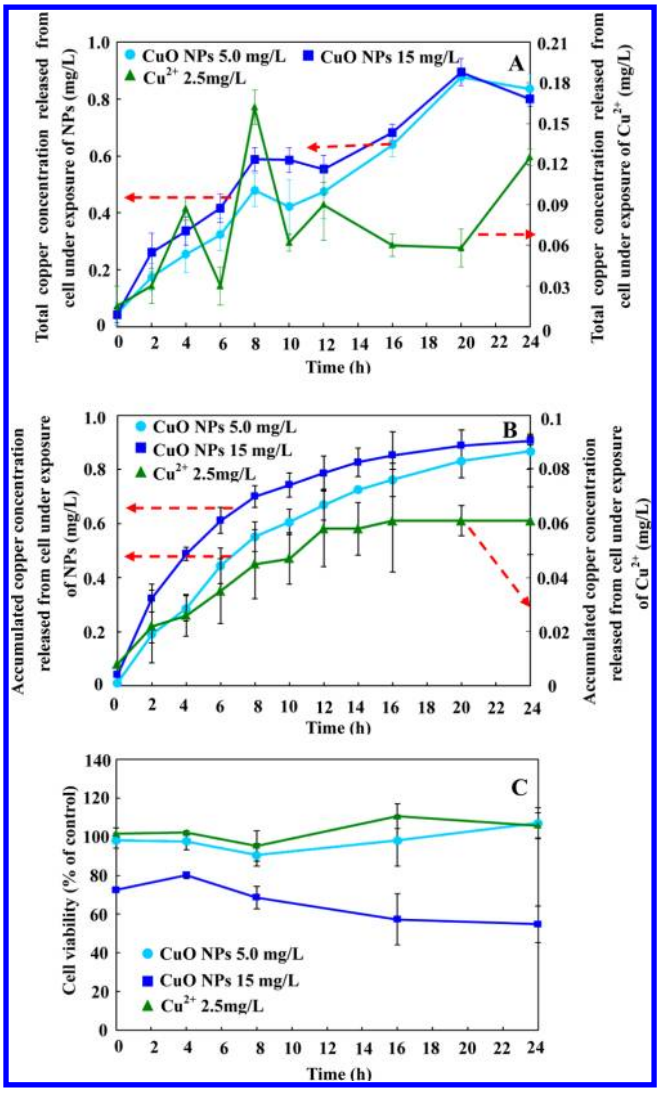

Figure 5. Export of internalized CuO NPs and Cu^{2+} ions by A549 cells. (A) A549 cells were incubated with CuO NPs (5 and 15 mg/L) or Cu^{2+} ions (2.5 mg/L) for 24 h, then washed, and incubated with fresh cell medium. The Cu concentration in the amended medium was determined after incubation of 2, 4, 6, 8, 10, 12, 16, 20, and 24 h. (B) A549 cells were incubated with CuO NPs (5 and 15 mg/L) or Cu^{2+} ions (2.5 mg/L) for 24 h, washed, and incubated with the fresh cell medium, and then, the cell medium was replaced with fresh medium at different time intervals (2, 4, 6, 8, 10, 14, 16, 20, and 24 h). The Cu concentration of the cell medium after incubation was determined, and the accumulated copper concentration released from cell was calculated. (C) Kinetics of cell viability. The cells were incubated with CuO NPs (5 and 15 mg/L) or Cu^{2+} ions (2.5 mg/L) for 24 h, washed, and incubated with fresh cell medium for 0−24 h. Panels A and B both have a double *Y*-axis, and each curve and its respective *Y*-axis is indicated by a red arrow. Data represent mean values ± standard deviations (n = 3).

CuO NP aggregates were observed in the cell medium (Figure S9 in the Supporting Information), suggesting that the excreted Cu was in the form of both dissolved Cu^{2+} ions and NPs.

To make sure whether the injured cells could return to normal level during CuO NP export, cell viability during CuO NP export was measured (Figure 5C). For cells pretreated with 5 mg/L CuO NPs and 2.5 mg/L Cu^{2+}, the viability did not change as compared to the control, indicating that the excretion process could partially alleviate the toxicity of low-concentration CuO NPs (5 mg/L) and Cu^{2+} ions (2.5 mg/L). However, at 15 mg/L CuO NPs, the cell viability first increased during initial 4 h, then decreased significantly, and stabilized at about 50% ($p < 0.05$). Although a fraction of Cu NPs (or Cu^{2+} ions) was exported from cells, the cell viability after CuO NPs (15 mg/L) exposure was low, probably due to the greater extent of cell damage (cell membrane damage, mitochondrial depolarization, and DNA damage) as described above. Moreover, the membrane damage as indicated by the LDH assay (Figure S7 in the Supporting Information) could also contribute to the export of Cu^{2+} ions and NPs.

Contribution of Dissolved Cu^{2+} on CuO NPs Toxicity. The Cu^{2+} ions on cell membrane damage, ROS production, mitochondrial depolarization, and DNA damage was measured to quantitative understanding on the effect of released Cu^{2+} ions from CuO NPs on the total toxicity. The toxicity contribution percentage of Cu^{2+} ions to CuO NPs was calculated. After 24 h of exposure to 15 mg/L CuO NPs, Cu^{2+} ions contributed 31% of membrane damage and 27% of DNA damage caused by metal oxide NP exposure. After CuO NP (15 mg/L) exposure for 2 h, Cu^{2+} ions contributed 47 and 46% of total ROS generation and mitochondrial depolarization levels, respectively. Therefore, dissolved Cu^{2+} ions contributed to less than 50% of the overall cytotoxicity from CuO NP exposure. Midander et al. reported that Cu^{2+} ions dissolved from CuO NPs caused insignificant DNA damage and contributed a lower percentage of the overall toxicity to A549 cells than our finding.[50] This could attribute to the much shorter exposure time in that study (4 h) relative to our study (24 h).

In summary, CuO NPs were clearly observed in both the cell nucleus and the mitochondria. CuO NPs were taken up by A549 cells mainly through endocytosis, although part of the internalized CuO NPs were dynamically excreted to the extracellular environment. Deposition of CuO NPs in mitochondria resulted in ROS generation, ultimately inducing mitochondrial depolarization. CuO NPs induced robust ROS production, and expression of *p38* and *p53* was significantly up regulated, resulting in irreversible DNA damage. Oxidative stress was confirmed to be the first response of CuO NPs cytotoxicity, rather than DNA damage. Moreover, free Cu^{2+} and protein-bound Cu^{2+} released from CuO NPs in cell medium were accurately evaluated using centrifugal ultrafiltration tubes. The contribution of Cu^{2+} ions dissolved from CuO NPs in the cell medium was less than 50% of the total observed cytotoxicity. These data clearly show that increased attention and careful investigations are needed regarding potential exposure, toxicity, and ultimate risk from metal oxide NPs such as CuO.

■ ASSOCIATED CONTENT

Ⓢ Supporting Information

Additional figures and tables. This material is available free of charge via the Internet at http://pubs.acs.org.

■ AUTHOR INFORMATION

Corresponding Author

*Tel: +1-413-545-5212. Fax: +1-413-545-3958. E-mail: bx@pssci.umass.edu (B.X.); E-mail: wang0628@ouc.edu.cn (Z.W.).

Funding

This work is supported by the Natural Science Foundation of China (41073067, 41120134004) and USDA-AFRI Hatch program (MAS 00978).

Notes

The authors declare no competing financial interest.

■ ABBREVIATIONS

NPs, nanoparticles; A549 cell line, human lung epithelial cells; F12K, nutrient mixture F12 Ham Kaighn's modified medium; FBS, fetal bovine serum; BPs, bulk particles; TEM, transmission electron microscopy; CCK-8, cholecystokinin octapeptide; IC_{50}, half maximal inhibitory concentration; FAAS, flame atomic absorption spectrometry; GAAS, graphite furnace-atomic absorption spectrometry; EDS, energy dispersive spectroscopy; EB, ethidium bromide; PBS, phosphate buffer solution; DCF-DA, 2,7-dichlorodihydrofluo-rescein diacetate; FI, fluorescence intensity; ROS, reactive oxygen species; MMP, mitochondrial membrane potentials; JC-1, 5,5′,6,6′-tetrachloro-1,1′,3,3′-tetraethyl-imidacarbocyanine iodide; RT-PCR, real-time polymerase chain reaction; Comet assay, alkaline single-cell gel electrophoresis; LDH, lactase dehydrogenase; NPCs, nuclear pore complexes; NRs, nanorods

■ REFERENCES

(1) Serpone, N., Dondi, D., and Albini, A. (2007) Inorganic and organic UV filters: their role and efficacy in sunscreens and suncare products. *Inorg. Chim. Acta 360*, 794−802.

(2) Dutta, A., Das, D., Grilli, M., Di, B. E., Traversa, E., and Chakravorty, D. (2003) Preparation of solgel nano-composites containing copper oxide and their gas sensing properties. *J. Sol-Gel Sci. Technol. 26*, 1085−1089.

(3) Prinz, G. A. (1999) Magnetoelectronics. *Science 283*, 330−330.

(4) Kobe, S., Drazic, G., McGuiness, P. J., and Strazisar, J. (2001) The influence of the magnetic field on the crystallisation form of calcium carbonate and the testing of a magnetic water-treatment device. *J. Magn. Magn. Mater. 236*, 71−76.

(5) Xia, T., Kovochich, M., Liong, M., Madler, L., Gilbert, B., Shi, H., Yeh, J. I., Zink, J. I., and Nel, A. E. (2010) Comparison of the mechanism of toxicity of zinc oxide and cerium oxide nanoparticles based on dissolution and oxidative stress properties. *ACS Nano 2*, 2121−2134.

(6) Maurer-Jones, M. A., Lin, Y., and Haynes, C. L. (2010) Functional assessment of metal oxide nanoparticle toxicity in immune cells. *ACS Nano 4*, 3363−3373.

(7) Xia, T., Kovochich, M., Brant, J., Hotze, M., Sempf, J., Oberley, T., Sioutas, C., Yeh, J. I., Wiesner, M. R., and Nel, A. E. (2006) Comparison of the abilities of ambient and manufactured nano-particles to induce cellular toxicity according to an oxidative stress paradigm. *Nano Lett. 6*, 1794−1807.

(8) Yang, H., Liu, C., Yang, D., Zhang, H., and Xi, Z. (2009) Comparative study of cytotoxicity, oxidative stress and genotoxicity induced by four typical nanomaterials: the role of particle size, shape and composition. *J. Appl. Toxicol. 29*, 69−78.

(9) AshaRani, P. V., Low Kah Mun, G., Hande, M. P., and Valiyaveettil, S. (2009) Cytotoxicity and genotoxicity of silver nanoparticles in human cells. *ACS Nano 3*, 279−290.

(10) Eom, H., and Choi, J. (2010) p38 MAPK activation, DNA damage, cell cycle arrest and apoptosis as mechanisms of toxicity of silver nanoparticles in Jurkat T cells. *Environ. Sci. Technol. 44*, 8337−8342.

(11) Geiser, M., Rothen-Rutishauser, B., Kapp, N., Schurch, S., Kreyling, W., Schulz, H., Semmler, M., Im Hof, V., Heyder, J., and Gehr, P. (2005) Ultrafine particles cross cellular membranes by nonphagocytic mechanisms in lungs and in cultured cells. *Environ. Health. Perspect. 113*, 1555−1560.

(12) Ahamed, M., Karns, M., Goodson, M., Rowe, J., Hussain, S. M., Schlager, J. J., and Hong, Y. (2008) DNA damage response to different surface chemistry of silver nanoparticles in mammalian cells. *Toxicol. Appl. Pharmacol. 233*, 404−410.

(13) Asati, A., Santra, S., Kaittanis, C., and Perez, J. M. (2010) Surface-charge-dependent cell localization and cytotoxicity of cerium oxide nanoparticles. *ACS Nano 4*, 5321−5331.

(14) Jiang, X., Röcker, C., Hafner, M., Brandholt, S., Dörlich, R. M., and Nienhaus, G. U. (2010) Endo- and exocytosis of zwitterionic quantum dot nanoparticles by live HeLa cells. *ACS Nano 4*, 6787−6797.

(15) Ma, Y., Kuang, L., He, X., Bai, W., Ding, Y., Zhang, Z., Zhao, Y., and Chai, Z. (2010) Effects of rare earth oxide nanoparticles on root elongation of plants. *Chemosphere 78*, 273−279.

(16) Wang, Z., Li, J., Zhao, J., and Xing, B. (2011) Toxicity and internalization of CuO nanoparticles to prokaryotic alga *microcystis aeruginosa* as affected by dissolved organic matter. *Environ. Sci. Technol. 45*, 6032−6040.

(17) Gunawan, C., Teoh, W. Y., Marquis, C. P., and Amal, R. (2011) Cytotoxic origin of copper(II) oxide nanoparticles: comparative studies with micron-sized particles, leachate, and metal salts. *ACS Nano 5*, 7214−7225.

(18) Zhao, J., Wang, Z., Liu, X., Xie, X., Zhang, K., and Xing, B. (2011) Distribution of CuO nanoparticles in juvenile carp (*Cyprinus carpio*) and their potential toxicity. *J. Hazard. Mater. 197*, 304−310.

(19) Karlsson, H. L., Cronholm, P., Gustafsson, J., and Möller, L. (2008) Copper oxide nanoparticles are highly toxic: a comparison between metal oxide nanoparticles and carbon nanotubes. *Chem. Res. Toxicol. 21*, 1726−1732.

(20) Simon-Deckers, A., Gouget, B., Mayne-L'Hermite, M., Herlin-Boime, N., Reynaud, C., and Carrière, M. (2008) In vitro investigation of oxide nanoparticle and carbon nanotube toxicity and intracellular accumulation in A549 human pneumocytes. *Toxicology 253*, 137−146.

(21) Braydich-Stolle, L. K., Speshock, J. L., Castle, A., Smith, M., Murdock, R. C., and Hussain, S. M. (2010) Nanosized aluminum altered immune function. *ACS Nano 4*, 3661−3670.

(22) Jugan, M. L., Barillet, S., Simon-Deckers, A., Sauvaigo, S., Douki, T., Herlin, N., and Carrière, M. (2011) Cytotoxic and genotoxic impact of TiO_2 nanoparticles on A549 cells. *J. Biomed. Nanotechnol. 7*, 22−23.

(23) Wang, L., Liu, Y., Li, W., Jiang, X., Ji, Y., Wu, X., Xu, L., Qiu, Y., Zhao, K., Wei, T., et al. (2011) Selective targeting of gold nanorods at the mitochondria of cancer cells: implications for cancer therapy. *Nano Lett. 11*, 772−780.

(24) Navarro, E., Piccapietra, F., Wagner, B., Marconi, F., Kaegi, R., Odzak, N., Sigg, L., and Behra, R. (2008) Toxicity of silver nanoparticles to *chlamydomonas reinhardtii*. *Environ. Sci. Technol. 42*, 8959−8964.

(25) Franklin, N. M., Stauber, J. L., Markich, S. J., and Lim, R. P. (2000) pH-dependent toxicity of copper and uranium to a tropical freshwater alga (*Chlorella sp.*). *Aquat. Toxicol. 48*, 275−289.

(26) Fisher, H. W., and Harris, H. (1962) The isolation of nuclei from animal cells in culture. *Proc. R. Soc. London B 156*, 521−523.

(27) Tan, C., Lai, S., Wu, S., Hu, S., Zhou, L., Chen, Y., Wang, M., Zhu, Y., Lian, W., Peng, W., Ji, L., and Xu, A. (2010) Nuclear permeable ruthenium(II) β-carboline complexes induce autophagy to antagonize mitochondrial-mediated apoptosis. *J. Med. Chem. 53*, 7613−7624.

(28) Zhang, C., Zhu, H., Yang, X., Lou, J., Zhu, D., Lu, W., He, Q., and Yang, B. (2010) p53 and p38 MAPK pathways are involved in MONCPT-induced cell cycle G2/M arrest in human non-small cell lung cancer A549. *J. Cancer Res. Clin. Oncol. 136*, 437−445.

(29) Livak, K. J., and Schmittgen, T. D. (2001) Analysis of relative gene expression data using real-time quantitative PCR and the 2-ΔΔCT method. *Methods 25*, 402−408.

(30) Singh, N. P., McCoy, M. T., Tice, R. R., and Schneider, E. L. (1988) A Simple technique for quantitation of low levels of DNA damage in individual cells. *Exp. Cell Res. 175*, 184−191.

(31) Sharma, V., Shukla, R. K., Saxena, N., Parmar, D., Das, M., and Dhawan, A. (2009) DNA damaging potential of zinc oxide nanoparticles in human epidermal cells. *Toxicol. Lett. 185*, 211−218.
(32) Chithrani, B. D., and Chan, W. C. W. (2007) Elucidating the mechanism of cellular uptake and removal of protein-coated gold nanoparticles of different sizes and shapes. *Nano Lett. 7*, 1542−1550.
(33) Herd, H. L., Malugin, A., and Ghandehari, H. (2011) Silica nanoconstruct cellular toleration threshold in vitro. *J. Controlled Release 153*, 40−48.
(34) Huang, M., Khor, E., and Lim., L. Y. (2004) Uptake and cytotoxicity of chitosan molecules and nanoparticles: effects of molecular weight and degree of deacetylation. *Pharm. Res. 21*, 344−353.
(35) Kim, J. S., Yoon, T. J., Yu, K. N., Noh, M. S., Woo, M., Kim, B. G., Lee, K. H., Sohn, B. H., Park, S. B., Lee, J. K., et al. (2006) Cellular uptake of magnetic nanoparticle is mediated through energy-dependent endocytosis in A549 cells. *J. Vet. Sci. 7*, 321−326.
(36) Karlsson, H. L., Gustafsson, J., Cronholm, P., and Möller, L. (2009) Size-dependent toxicity of metal oxide particles—A comparison between nano- and micrometer size. *Toxicol. Lett. 188*, 112−118.
(37) Yang, S. T., Liu, J. H., Wang, J., Yuan, Y., Cao, A., Wang, H., Liu, Y., and Zhao, Y. (2010) Cytotoxicity of zinc oxide nanoparticles: Importance of microenvironment. *J. Nanosci. Nanotechnol. 10*, 8638−8645.
(38) Meng, H., Chen, Z., Xing, G., Yuan, H., Chen, C., Zhao, F., Zhang, C., and Zhao, Y. (2007) Ultrahigh reactivity provokes nanotoxicity: Explanation of oral toxicity of nano-copper particles. *Toxicol. Lett. 175*, 102−110.
(39) Muno, D., Sutoh, N., Watanabe, T., Uchiyama, Y., and Kominama, E. (1990) Effect of metabolic alterations on the density and the contents of cathepsins B, H and L of lysosomes in rat macrophages. *Eur. J. Biochem. l91*, 91−98.
(40) Macara, I. G. (2001) Transport into and out of the nucleus. *Microbiol. Mol. Biol. Rev. 65*, 570−594.
(41) Mu, Q., Broughton, D. L., and Yan, B. (2009) Endosomal leakage and nuclear translocation of multiwalled carbon nanotubes: developing a model for cell uptake. *Nano Lett. 9*, 4370−4375.
(42) Akey, C. W., and Radermacher, M. (1993) Architecture of the *xenopus* nuclear pore complex revealed by three-dimensional cryo-electron microscopy. *J. Cell Biol. 122*, 1−19.
(43) Vasu, S. K., and Forbes, D. J. (2001) Nuclear pores and nuclear assembly. *Curr. Opin. Cell Biol. 13*, 363−375.
(44) Liang, Y., Luo, F., Lin, Y., Zhou, Q., and Jiang, G. (2009) C_{60} affects DNA replication in vitro by decreasing the melting temperature of DNA templates. *Carbon 47*, 1457−1465.
(45) Zhao., X., Striolo, A., and Cummings, P. T. (2005) C_{60} binds to and deforms nucleotides. *Biophys. J. 89*, 3856−3862.
(46) Wang, Y., Aker, W. G., Hwang, H., Yedjou, C. G., Yu, H., and Tchounwou, P. B. (2011) A study of the mechanism of in vitro cytotoxicity of metal oxide nanoparticles using catfish primary hepatocytes and human HepG2 cells. *Sci. Total Environ. 409*, 4753−4762.
(47) Levraut, J.., Iwase, H.., Shao, Z. H., Vanden Hoek, T. L., and Schumacker, P. T. (2002) Cell Death during ischemia: Relationship to mitochondrial depolarization and ROS generation. *Am. J. Physiol. Heart Circ. Physiol. 284*, 549−558.
(48) Liu, Y., and Martin, M. (2001) p53 protein at the hub of cellular DNA damage response pathways through sequence-specific and non-sequence-specific DNA binding. *Carcinogenesis 22*, 851−860.
(49) Kang, S. J., Kim, B. M., Lee, Y. J., Hong, S. H., and Chung, H. W. (2009) Titanium dioxide nanoparticles induce apoptosis through the JNK/p38-caspase-8-Bid pathway in phytohemagglutinin-stimulated human lymphocytes. *Biochem. Biophys. Res. Commun. 386*, 682−687.
(50) Midander, K., Cronholm, P., Karlsson, H. L., Elihn, K., Möller, L., Leygraf, C., and Wallinder, I. O. (2009) Surface characteristics, copper release, and toxicity of nano- and micrometer-sized copper and copper(II) oxide particles: A cross-disciplinary study. *Small 5*, 389−399.